AGU PUBLICATIONS

JGR

Journal of Geophysical Research: Oceans

RESEARCH ARTICLE

10.1002/2015JC010833

The deep circulation of the Faroe-Shetland Channel: Opposing flows and topographic eddies

Maria B. Broadbridge[1] and Ralf Toumi[1]

[1]Department of Physics, Imperial College, London, UK

Key Points:
- Existence of northeastward flow in the deep western Faroe-Shetland Channel
- Eddies force the deep currents into a gyre-like circulation
- Float and tracer release experiments suggest two main flow regimes

Correspondence to:
M. B. Broadbridge,
m.broadbridge@imperial.ac.uk

Citation:
Broadbridge, M. B., and R. Toumi (2015), The deep circulation of the Faroe-Shetland Channel: Opposing flows and topographic eddies, *J. Geophys. Res. Oceans*, *120*, 5983–5996, doi:10.1002/2015JC010833.

Received 11 MAR 2015
Accepted 14 AUG 2015
Accepted article online 18 AUG 2015
Published online 4 SEP 2015

The copyright line for this article was changed on 20 NOV 2015 after original online publication.

Abstract New insights into the deep circulation of the Faroe-Shetland channel are gained from a high-resolution regional ocean model. The simulation shows a more complex structure of the deep flow field than previously thought: a flow reversal of the deep and intermediate waters to the northeast on the Faroese flank of the channel and persistent topographic eddies that force the deep currents into a gyre-like structure. This flow reversal opposes the previously accepted understanding of a purely southwestward deep flow but is in agreement with velocity measurements. The southwestward transport of the overflow waters is found to be facilitated almost exclusively by a strong and narrow current on the Shetland side of the channel. Float release experiments show that up to 38% of the overflow water takes longer than a purely southwestward flow regime suggests and up to 13% takes twice as long. From the release of tracers, a substantial amount of lateral mixing is evident within the channel, predominantly facilitated by the topographic eddies.

1. Introduction

The marginal seas in the northernmost part of the Atlantic Ocean play a fundamental role in the transfer of water masses between the Arctic Seas and the North Atlantic, which is a key driver of the Atlantic Meridional Overturning Circulation. Cold, dense water flowing southward from high latitudes is inhibited by the Greenland-Scotland Ridge, which forms a barrier with only few passages deep enough to allow overflow into the North Atlantic.

One of the main pathways of this water mass exchange is the Faroe-Shetland Channel (FSC, Figure 1), a deep trough running between the Faroe Islands and Shetland in a southwestward direction, bounded by the Wyville-Thomson Ridge before turning to the northwest into the Faroe Bank Channel (FBC). The upper currents of the FSC carry just under half the total mass flux and just over half the total heat transport of Atlantic origin into the Arctic [*Hansen and Østerhus*, 2000]. An estimated volume transport of 2.1 Sv (1 Sv (Sverdrup) = 10^6 m^3s^{-1}) of colder and fresher waters from the Nordic seas and the Arctic Ocean return through the channel below about 500 m depth, forming the return flow of the thermohaline circulation [e.g., *Olsen et al*., 2008]. Approximately 0.3 Sv overflow across the Wyville-Thomson Ridge into the Rockall Trough [*Sherwin et al*., 2008] which has a sill depth of between 500 and 600 m with the remainder entering the Iceland Basin through the FBC.

While the nature of the Atlantic inflow has been extensively studied and reviewed, most recently in a comprehensive study by *Berx et al*. [2013], there are far fewer studies that examine the deep circulation in the FSC. The currently accepted picture of the mean currents in the deep FSC assumes a unidirectional path of the overflow waters to the southwest [e.g., *Dooley and Meincke*, 1981; *Sherwin et al*., 2006]. The deepest currents containing the densest waters, namely the Arctic Intermediate Water (AIW) and the Nordic Seas Deep Water (NSDW), flow southwestward through the FSC and exit mainly through the FBC into the North Atlantic. The deepest intermediate waters, the Modified East Icelandic Water (MEIW), also flow southwestward along the Faroese shelf and return northeastward along the Shetland shelf after being deflected back into the channel at the Wyville-Thomson Ridge.

Sherwin et al. [2006] indicate the possibility of a northeastward current on the deep Faroese flank of the channel by estimating geostrophic currents from two CTD sections across the FSC, the authors however maintain the view that the flow in the deep is as described in the preceding paragraph. The present study challenges this and provides a novel view of the deep currents in the FSC. By using a regional ocean model

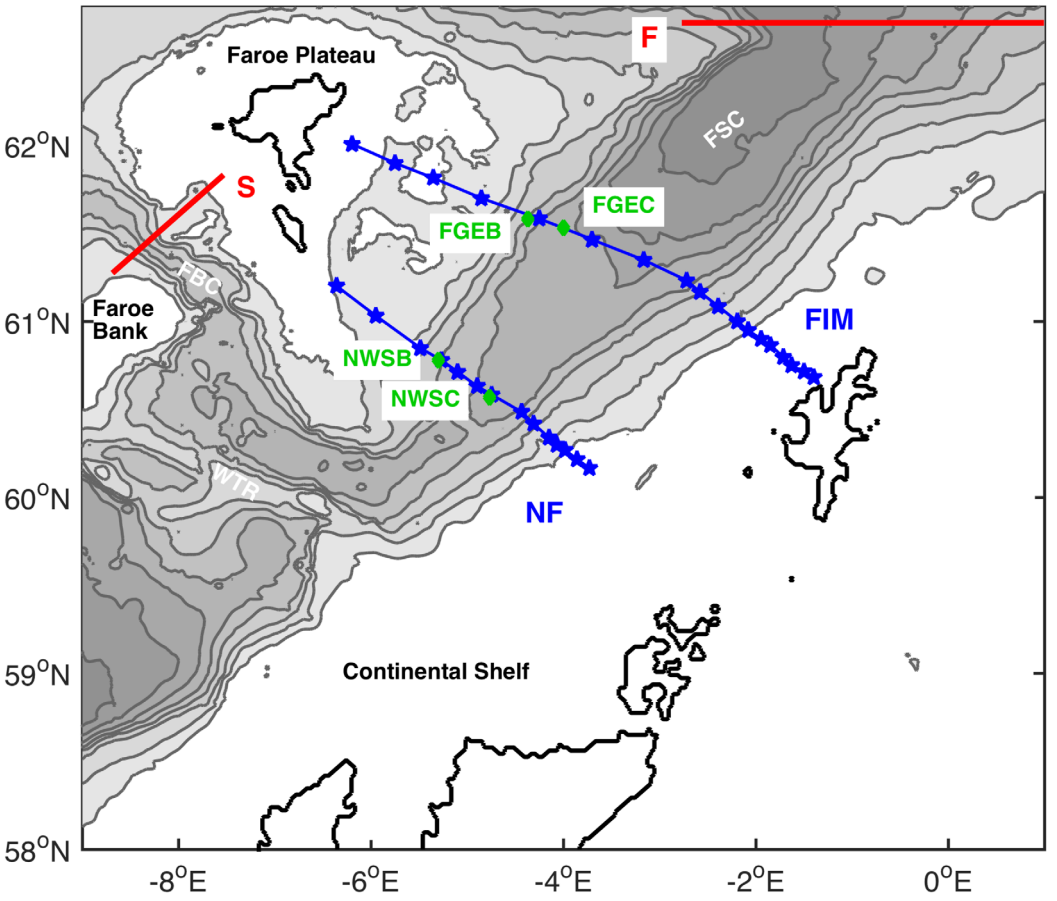

Figure 1. Model domain with bathymetry in grey shading (grey isobaths: 200 m spacing, black coastlines: 0 m depth). The red lines denote the Faroe Bank Channel section (S) and the numerical float release sites (F). ADCP stations (NWSB, NWSC, FGEB, and FGEC) are marked by green diamonds and the standard CTD stations (Fair Isle-Munken Section (FIM) and Nolsoy-Flugga Section (NF)) by blue stars.

with realistic bathymetry and boundary conditions which is described in the following section, the ocean in the region of the FSC is simulated and reveals a significantly more complex structure of the deep circulation, with a significant portion of the deep mean flow directed to the northeast. This is confirmed by comparisons with ADCP current measurements at selected locations. Float and tracer release experiments elucidate the pathways which water parcels take while passing through the channel and how persistent topographic eddies split the flow into two main regimes: a fast southwestward current near the Shetland shelf and an intensely mixed recirculation region in the remainder of the channel. The key results are then discussed and followed by a brief conclusion.

2. Methodology

2.1. Model Setup

To simulate the ocean in the region of the Faroe-Shetland Channel, the Regional Ocean Modelling System (ROMS; COAWST svn version 790), which is a free-surface, hydrostatic, primitive equation ocean model [*Shchepetkin and McWilliams*, 2005; *Haidvogel et al*., 2008; *Shchepetkin and McWilliams*, 2009], is used. The model domain, shown in Figure 1 is on a regular Cartesian grid with a horizontal resolution of approximately 2 km and extends from 58°N to 62.8°N and −9°E to 1°E. The vertical structure yields 35 depth levels of variable spacing in the vertically stretched terrain-following ROMS σ coordinate over realistic bottom topography from satellite altimetry and ship depth soundings [*Smith and Sandwell*, 1997]. Three-dimensional advection of momentum is discretized with a third-order upstream bias horizontal advection scheme with a velocity-dependent Smagorinsky-like viscosity [*Smagorinsky*, 1963] and a fourth-order centered vertical advection scheme. For the advection of tracers, the nonoscillatory MPDATA algorithm is used.

Subgrid-scale mixing of mass and momentum is parameterized using the generic length-scale (GLS) mixing scheme [*Warner et al*., 2005] with horizontal smoothing of buoyancy and shear applied.

To initialize the model and force it at its boundaries, a monthly mean climatology containing sea level height, temperature, horizontal current velocities, and salinity from the 0.5° Simple Ocean Data Assimilation (SODA) [*Carton et al*., 2000] is implemented. The boundaries are forced by radiation conditions on outflow and nudging to the climatology values on inflow through a sponge layer which extends approximately 14 km into the model domain a tapering nudging time scale of 3 days at the boundary to 90 days in the model interior. This sponge layer has been applied to all four boundaries in order to provide a tapering of the circulation in the model interior to the boundary forcing. Tidal forcing at the boundary is obtained from the Oregon State University inverse tidal atlas of the Atlantic Ocean at 1/12° resolution (http://volkov.oce.orst.edu/tides/atlas.html). Atmospheric forcing at the surface is provided in form of downward longwave and shortwave radiation, mean sea level pressure, 2 m specific humidity, 2 m air temperature, 10 m winds, total cloud cover, and total precipitation by the NCEP Climate Forecast System Reanalysis (CFSR) [*Saha et al*., 2010].

Current speed and direction from the model output are compared to time series of broadband acoustic doppler profiler (ADCP) current measurements on the Faroese flank of the channel. The data were collected by the Faroese Fisheries Laboratory in the period October 1994 to June 2000 at fixed mooring sites within the Faroe-Shetland Channel. Details of the southern ADCP stations (NWSB, NWSC) of this data set are described by *Hughes et al*. [2005] and the northern stations (FGEB, FGEC) by *Larsen et al*. [2000].

To verify the distribution of water masses in the model interior, data from two standard CTD sections, namely the Fair Isle-Munken section (FIM) and the Nolsoy-Flugga section (NF) were used. An extensive description of these Faroese standard sections 1988–2010 is provided by *Larsen et al*. [2012]. The data are readily available from the British Oceanographic Data Centre.

3. ROMS Experiments

3.1. The Model Spin-Up and Validation

The simulation of the FSC currents is initialized in January 1994 and run for a total of 9 years. The first 3 years are used to spin-up the model, and from January 1997, the model results of the remaining 6 years are analyzed and the float and tracer release experiments are carried out. This time frame is specifically chosen to overlap with the observations used for model verification.

To visualize the horizontal structure of the deep circulation, the model results are interpolated onto three isosurfaces of 600, 750, and 900 m depth. These depths are chosen because they encompass the deepest water masses within the channel and elucidate the horizontal structure of the deep flow. Figure 2 shows the mean currents averaged for the period 1997–2002. The main features are an intense and narrow southwestward current that flows along the slope on the Shetland shelf, gets deflected and amplified in strength by a cyclonic vortex that resides in the narrowest part of the channel mouth and then exits in meanders through the FBC. This current is most intense on the 750 m surface and weaker on both the 600 and 900 m surface.

The remainder of the channel interior is dominated by eddies. Two sizeable anticyclonic vortices are located at the entrance and appear to direct the currents either toward the slope current or out of the channel. They have a similar shape and structure on all three isosurfaces. Further southward within the channel, a number of smaller vortices are located, which change in shape across the isosurfaces. On the Faroese half of the FSC, the currents are predominantly flowing to the north-east.

The stratification of the model is compared to that of two standard CTD sections, which are denoted by the blue stars in Figure 1. The NF section crosses the northern part of the FSC while the FIM section is located to the south. Data from those sections have been widely published [e.g., *Turrell et al*., 1999] and shall not be discussed here in detail. Temperature data from both sections during occupations in May, October, and December 2004–2006 were used to estimate the mean across-channel buoyancy frequency and averaged over each of the months of the occupation periods (blue profiles in Figure 3a). The same method was applied to the model data (red profiles in Figure 3a). The results show that while the magnitude of the buoyancy frequency is similar between model and observations, the peak of the stratification at middepth, which is the intercepting region between the shallow waters from the North Atlantic and the dense nordic

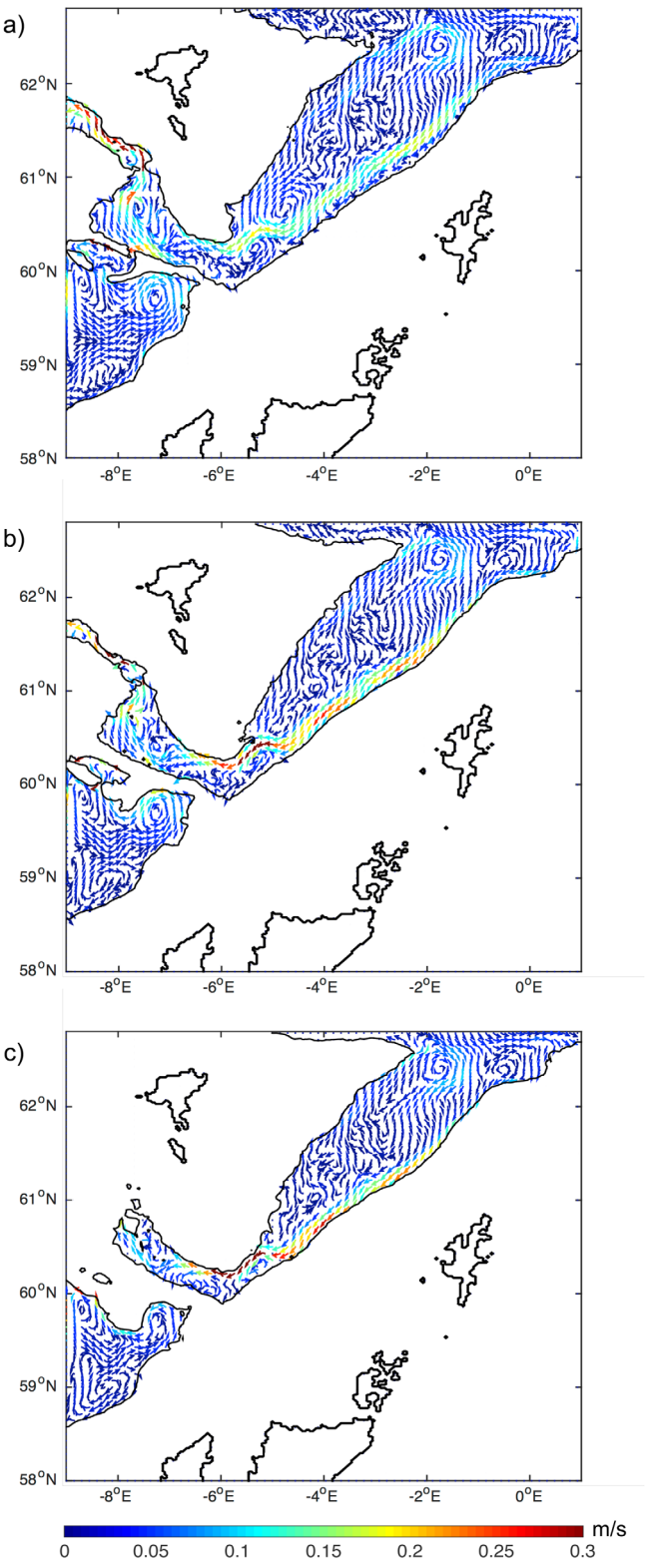

Figure 2. The mean model circulation averaged for the period 1997–2002 on the (a) 600 m, (b) 750 m, and (c) 900 m depth isosurface. Land is contoured black for reference. Vector arrows denote the current direction and their colors the current speed in meter per second.

water masses, lies deeper in the model results. This is further confirmed by comparing the mean model density at the FIM section (Figure 3b), averaged over 1997–2002 to known conditions in the FSC (Figure 3b) [*Berx et al.*, 2013]. The figure shows a greater abundance of water masses lighter than 27.5 kg m^{-3} in the model result and slightly less waters with densities greater than 28 kg m^{-3}.

To verify the existence of this north/northeastward component of the flow, the model results are compared to ADCP current data. The data set comprises nine ADCP locations in total, four of which were used in the present study. Of all the stations, four were discarded because they are outside of the FSC, three of which are located north of Faroe and one near the exit of the FBC. One further station was discarded for this study because it is located in too shallow waters on the Faroese shelf with a maximum depth of about 293 m. Since this study investigates the deep currents of the FSC, only stations with measurements deeper than 500 m are considered, namely NWSB, NWSC, FGEB, and FGEC. Diamonds in Figure 1 show the locations of those four ADCP stations which are located in depth within currents that are thought to be directed to the southwest but a substantial portion is found to be predominantly northeastward in this study. The ADCP data have been collected with a sampling frequency of 5–20 min intervals in the time periods 23 October 1994 to 20 June 2000 (NWSB, NWSC) and 21 February 1999 to 17 June 2000 (FGEB, FGEC). In order to compare them with the model data and to eliminate the variability of the diurnal tide in this region, 24 hourly averaging has been applied to both model and ADCP data. Periods in which no data were available from the current meters have been removed from the data set. Results closest to (always within 5 m) the 620 m depth bin are shown for all available data in Figure 4 in form of a compass. This is the deepest depth

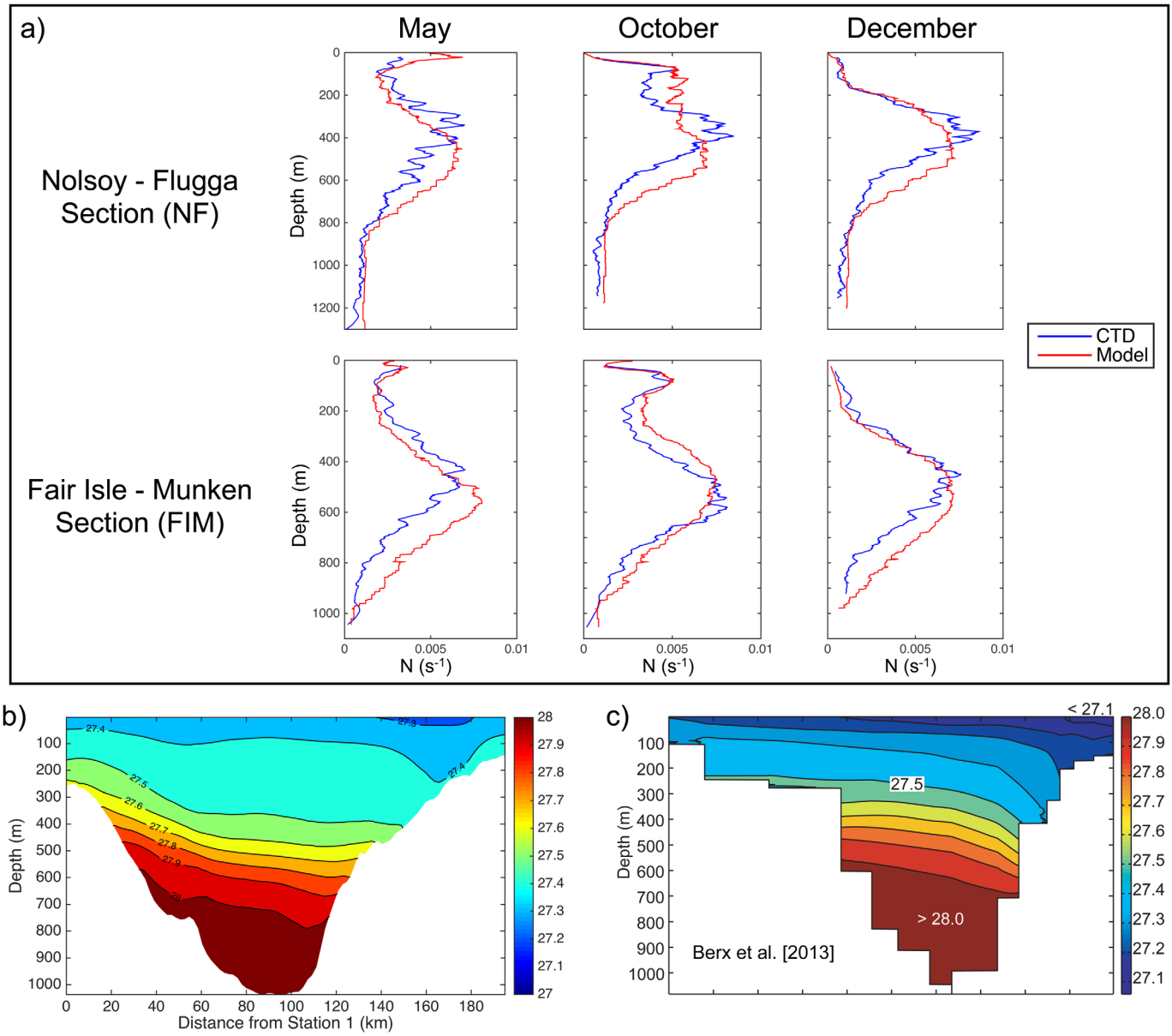

Figure 3. Comparison between CTD data and model results: (a) the mean across-channel buoyancy frequency for both CTD sections averaged for the time period 2004–2006, and the mean density (kg m^{-3}) at the Fair Isle-Munken section for (b) the model result, averaged for the period 1997–2002 and (c) from *Berx et al.* [2013, Figure 4c], 1995–2009 average.

bin that exists for all four ADCP stations in the FSC with the exception of one period of deeper measurements between 695 and 995 m at NWSC station for the period 1 August 1997 to 15 June 1998 which is shown separately in Figure 5. Color shading denotes the magnitude of the current speed and each data point is placed so it shows the current direction on the compass. The percentages, which are placed in the southwestern and northeastern corners of the plots in both Figures 4 and 5, denote how much of the current data occupy the southwestern and the northeastern quadrant of the compass compared to the full data set. This allows a direct comparison between the two opposing flows and shows which current direction dominates for all stations.

The currents in Figure 4 show a very clear result: the flow is not purely southwestward and a substantial portion of it is directed toward the northeast. While the ROMS model tends to underestimate the current speed, the direction of the current is broadly consistent with that of the data sets for all stations. The model currents show a greater variability in current direction than the ADCP data, which are shown in the overall

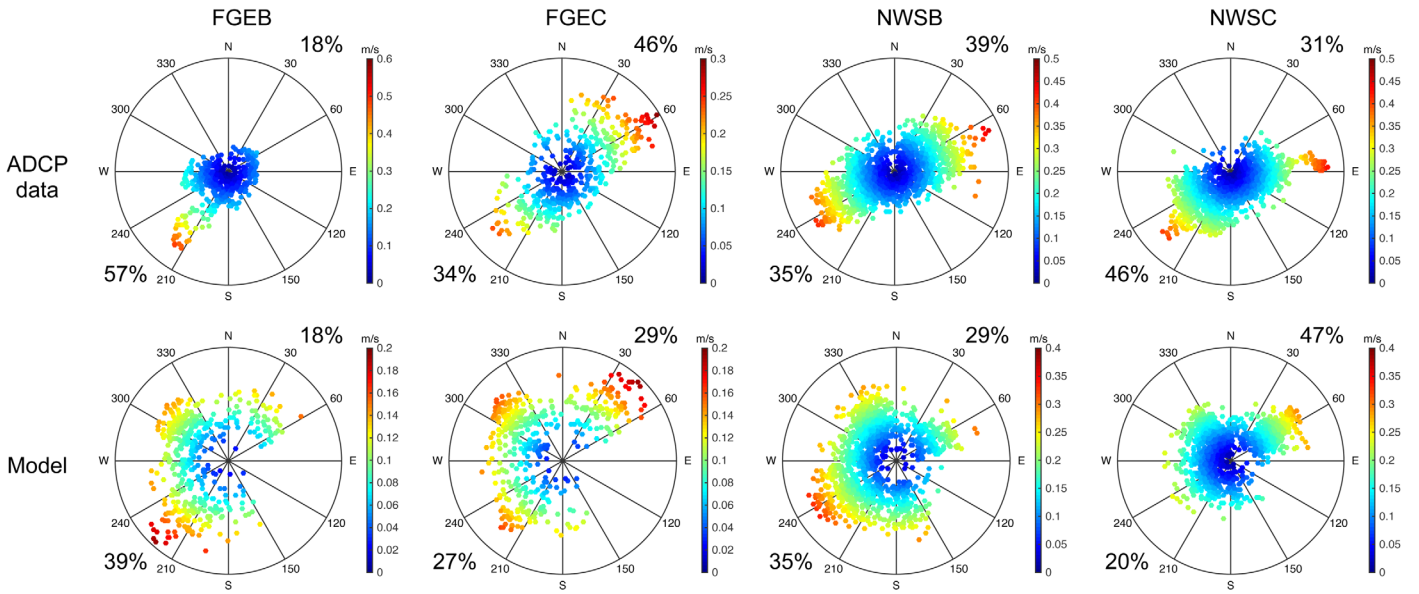

Figure 4. (top row) The daily mean current speed and direction for the ADCP stations and (bottom row) model results at the corresponding locations for all available data at 620 m depth during the time periods 21 February 1999 to 17 June 2000 (FGEB, FGEC) and 23 October 1994 to 20 June 2000 (NWSB, NWSC). The percentages on the lower left of each plot show the amount of data points located in the quadrant between 180° and 270° (southwestward flow) and those on the upper right the amount of data in the quadrant between 0° and 90° (northeastward flow).

lower percentages of the southwestern and northeastern flow components. At FGEB and NWSC, the greatest part of the current is directed to the southwest in the data set, which is confirmed by the model at FGEB but opposed at NWSC, where the model currents are predominantly northeastward. The opposite is true at FGEC, the data set shows substantial directional variability with the greatest amount of data points occupying the northeastern half of the compass. The model currents at this station are more evenly split between the northeastern and southwestern directions, with the greater component of the flow also directed to the northeast. At NWSB the current data show an almost equal flow in both directions with a dominance to the northeast whereas the model shows a larger component to the southwest.

To verify whether deeper currents behave in a similar fashion to those shown at 620 m, the depth-averaged daily mean current at NWSC station between 695 and 995 m is shown in Figure 5. There is almost no directional variability with depth and very little difference in current speed in the data set; hence, a depth average is shown rather than a series of figures with similar results for each depth. The currents in this figure are consistent with those in Figure 4 at NWSC station. This similarity between those deep ADCP data and those at 620 m confirms that the currents shown both figures must be part of the same currents, below the pycnocline, otherwise a significant difference in both current speed and direction should be expected.

3.2. Floats

To track the pathways of water parcels through the FSC, Lagrangian floats were released at every grid point north of the channel entrance between −2.7°E and 1°E at a latitude of 62.7°N and a depth of 750 m, which is shallow enough that it exists in both the FSC and FBC but deep enough so that it is located within the deepest main currents of the channel. The release sites are shown by the red line labeled "F" in Figure 1. The floats were released every 5 days for 1 year, amounting to 7373 floats in total, starting at the beginning of 1997 and the experiment was run for a total of 4 years until the end of 2000. Results for this entire period are considered. After this time, the floats were split into five main categories. Floats that did not enter the channel and were advected northward along the slopes were discarded and only those that crossed 61.4°N are considered in the results, leaving 4378 floats for analysis. The two main categories of interest are floats that are within the overflow waters and exit via the FBC or over the Wyville-Thomson Ridge. A part joins slope current and travel almost directly southwestward and the rest are floats that become trapped in eddies. Some floats are affected by the persistent eddies in such a way that their path turns northward before they reach the FBC or the Ridge and they return to the northern boundary. The last category constitutes a small number of floats that are still on the grid at the end of the experiment. They are trapped within the eddies and their fate is unknown.

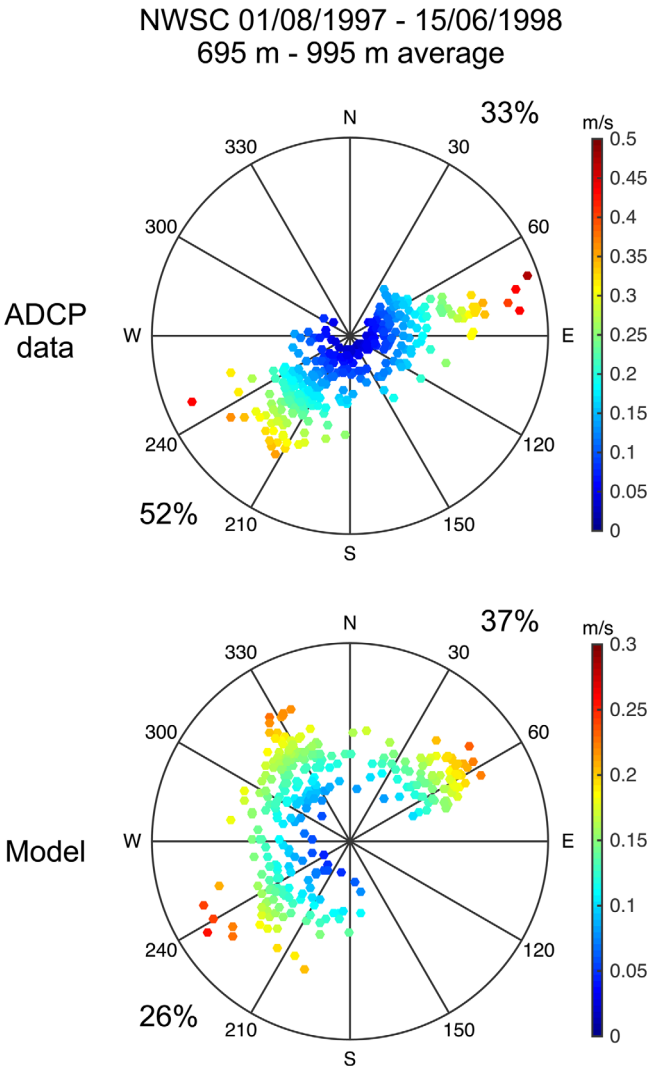

Figure 5. The depth-averaged daily mean current between 695 and 995 m is shown for the NWSC station during the time period 1 August 1997 to 15 June 1998 in the same style as Figure 4.

For comparison, floats from opposing ends of the time spectrum are shown in Figure 6: the path of the slowest float which takes 1349.2 days (almost 3.7 years) to reach the western edge of the grid (Figure 6a) and the fastest float with a passage time of 57.7 days (Figure 6b). In this experiment, the paths of the floats with a faster passage time than 115 days, apart from some meandering, do not significantly get altered by the eddies and they exit the channel by following the path of the slope current. These floats constitute 42% of the total number of floats that have entered the channel.

Floats released along the eastern portion of the line are more likely to be caught in the slope current and transported out of the channel quickly. The existence of the vortices at the channel entrance however modifies the path of the floats to such a degree that results from a separate analysis of the passage time between floats from the eastern and western part of the release site do not show much difference and shall not be discussed here.

The floats that are affected by the topographic eddies can be split into two subcategories. approximately 34.5% of the floats get recirculated by one or more of the eddies within the channel and exit to the south or southwest of the channel with a passage time between 115 and 1349.2 days. The rest of the floats, which constitute about 23.4% of the total number are those that return northward somewhere within the eddies and 14 floats (0.3%) which still remain on the grid after 4 years of simulation time.

The distribution density of the passage time between the floats that pass through the channel and exit via the FBC or the Wyville-Thomson Ridge is shown in Figure 6c in form of a histogram. The most common passage time is around the peak of about 87 days, which falls into the category of the floats whose path is mostly within the slope current. Most floats take longer than that, but the passage time is more variable, especially amongst those floats which are affected by eddies, where, for a time greater than about 170 days, only few floats have a common passage time. A lognormal probability distribution function (red line) is fitted in order to describe the distribution of the passage times which underestimates the peak in the distribution density and has a much thicker tail than the probability density of passage times longer than about 160 days suggests. A significantly better agreement over the peak data is obtained if the probability distribution is fitted over passage times with up to 240 days only (blue line).

The results of the passage time from the float experiment can be compared with observations of the volume transport of the overflow waters through the FBC. The time it would take to drain the FSC between

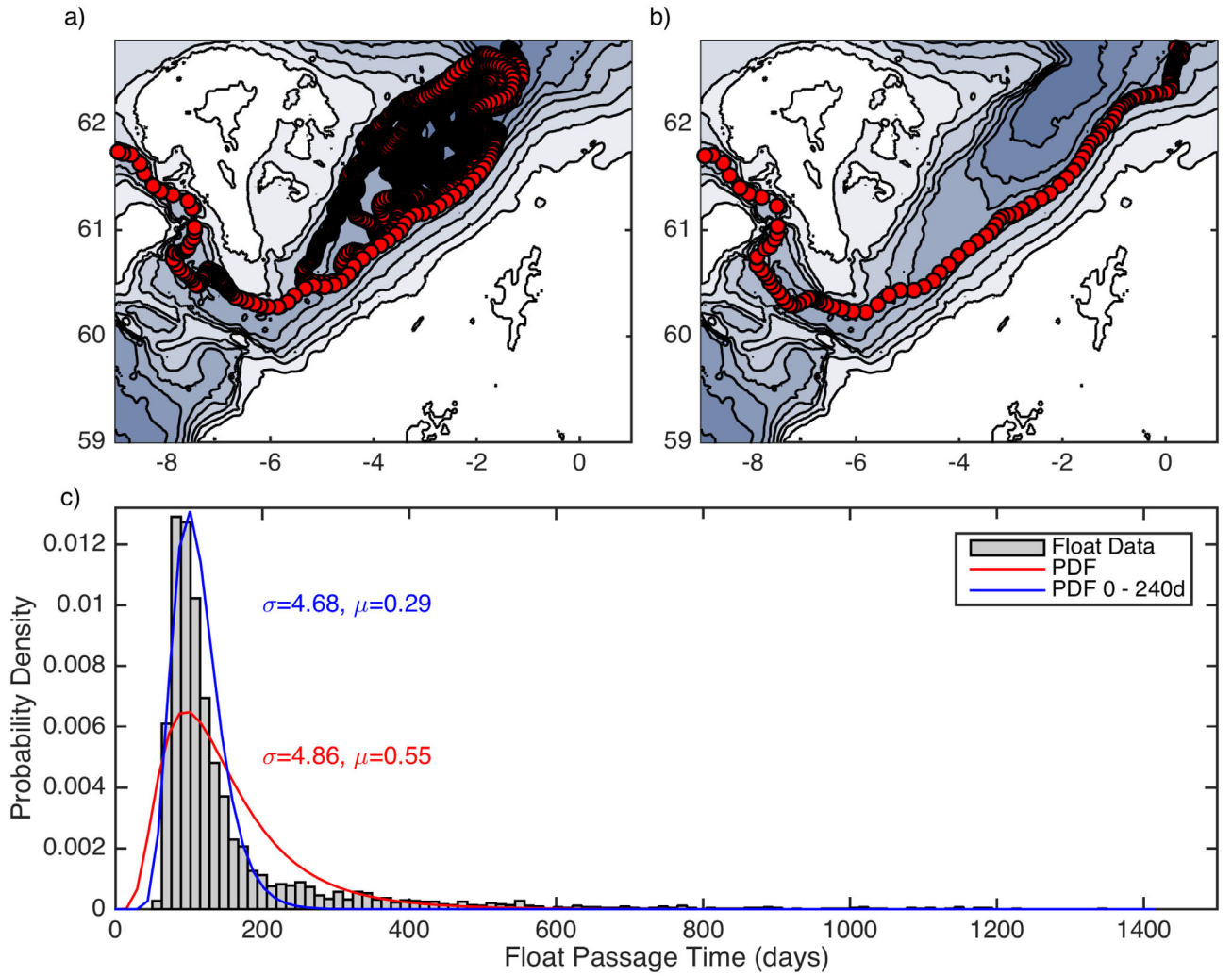

Figure 6. Float pathways are shown by red markers on the model bathymetry for (a) the slowest float and (b) the fastest float. The markers are spaced 12 h apart in time. (c) The probability density for the float passage time (histogram) and the corresponding fitted lognormal probability distribution functions (PDF). The red line shows the PDF for the full data set (p value = 0.078) while the blue line is fitted only to time scales shorter than 240 days (p value = 0.046). The mean μ and the standard deviation σ are shown in the respective colors of each PDF.

section F and S in Figure 1 below the depth of the interface between the inflowing and overflow waters can be estimated using equation (1) from observations which have been carried out at section S by various authors in the past.

$$t_{FBC} = \frac{V_{FSC}}{T_{vol}} \tag{1}$$

The drain time t_{FBC} is estimated from V_{FSC}, which is the volume of the channel below 550 m and the volume transport T_{vol} of the overflow waters across section S. The results are shown in Table 1. Comparing the results for the passage time of the floats to the drain time, we can estimate that 10%–38% of the floats in the model take longer than it would take to drain the deep FSC using the transports from the observations and the resulting ranges in drain time and 2%–13% take twice as long. The method and uncertainty of calculating this range in drain time is described in more detail in Appendix A. The broad range of the uncertainty comes from several sources of error which include the selection of the depth of the interface and the uncertainty in the observed transport measurements.

3.3. Tracers

For the tracer release experiment, the bottommost 20 layers of the water column north of the channel entrance were colored with a dye of an arbitrary initial concentration of 1. The dye is injected in a strip

Table 1. Estimated Volume Transport of the Overflow Waters Through the Faroe Bank Channel by Various Authors and the "Drain-Time" Calculated Using Equation (1)

Authors	Method	Transport (T_{vol}) (Sv)	Drain Time (t_{FBC}) (days)
Dooley and Meincke [1981]	Water masses	1.4	206–308
Borenäs and Lundberg [1988]	$T < 3°C$	1.7 ± 0.2	152–288
Saunders [1990]	$T < 3°C$	1.9 ± 0.4	125–288
Østerhus et al. [1999]	$T < 3°C$	1.9	152–228
Mauritzen et al. [2005]	$T < 3°C$	1.8 ± 0.2	145–270
Hansen and Østerhus [2007]	$T < 3°C$	1.9 ± 0.3	131–270

of one grid point width at a latitude of 62.7°N from the western boundary up until 0.4°E and at that longitude down to the southern boundary. This particular latitude was chosen to correspond with the numerical float release site and it ensured that all water that entered the channel from the northern boundary contained the dye, since layer depth is variable in the terrain-following ROMS σ coordinate and that the dye was not affected by sponge layers at the boundaries. The model was restarted on the 1 January 1997 with the initial dye concentration in those layers and run for a year. Results for this time frame are considered.

To interpret the results in terms of the model currents, the total tracer concentration is shown on the 750 m depth surface in Figure 7. Results for the tracer distribution after 30, 60, 90, and 120 days after the initialization time are considered. After 30 days, the dye has spread across most of the entrance of the channel concentrated on the Shetland side. The structure of the vortices in this region becomes apparent and the dye within the slope current has spread further south into the channel interior along the Shetland shelf slope. After 60 days, more dye is flushed southward by the slope current. Some has entered the FBC and is mixed by the ambient eddies. A part of the dye has started to join the recirculation in the currents on the Faroese side of the channel. The dye within the slope current still has the highest concentration, but mixing and entrainment of undyed water is apparent on the edges of the current. The vortex in the north of the channel has trapped and concentrated a significant amount of dye in its core. After 90 days, a significant amount of dye has been flushed out of the FBC and overflowed over the Wyville-Thomson Ridge, the concentration of the dye has decreased overall. The highest concentration resides within the two vortex cores in the north of the channel. The slope current appears to be transporting entrained undyed water south-westward and the northward flow on the Faroese flank of the channel is still almost dye free. After 120 days, the dye is mixed throughout the entire channel and undue water is starting to follow the flow pattern as seen in Figure 7a.

To elucidate the tracer results further, the time at which the tracer concentration first exceeds 0.001 or 0.1% of the initial concentration is shown in Figure 8. The reason for choosing such a low threshold concentration is to show a more complete picture of the horizontal circulation which captures both the slower and weaker recirculation branch as well as the swift dye transport in the narrow southwestward jet. Short threshold times (blue shading in Figure 8) denote areas where the dye is distributed quickly within the currents and longer threshold times (green to red shading in Figure 8) identify the areas of the channel which are reached slowly by the dye. This allows a clear distinction between the waters that feed the fast southwestward current and those that reside in the channel for a longer period of time

Three depth surfaces are shown: 600 m (Figure 8a), 750 m (Figure 8b), and 900 m (Figure 8c). The deepest surfaces show a similar distribution of the progression times for the tracer. The threshold concentration is reached fastest within the two vortices in the north of the channel and in the fast south-westward current. On the Faroese side of the channel, the threshold is reached after significantly longer time scales of up to 160 days in the recirculation region. At the shallower depth of 600 m, the pattern of the threshold time distribution is somewhat different to the deeper levels. The contours following the Shetland slope jet are broken up by longer threshold times whose contours appear to be connected to the recirculation region, suggesting the existence of a flow across the jet toward the Shetland slope.

The results of the tracer release experiments help to visually split the horizontal circulation clearly into the two flow regimes of slope-current transport and recirculating flow. They provide a map of the distribution and amount of deep FSC waters which occupy those regimes and show a clearer picture of the horizontal flow structure.

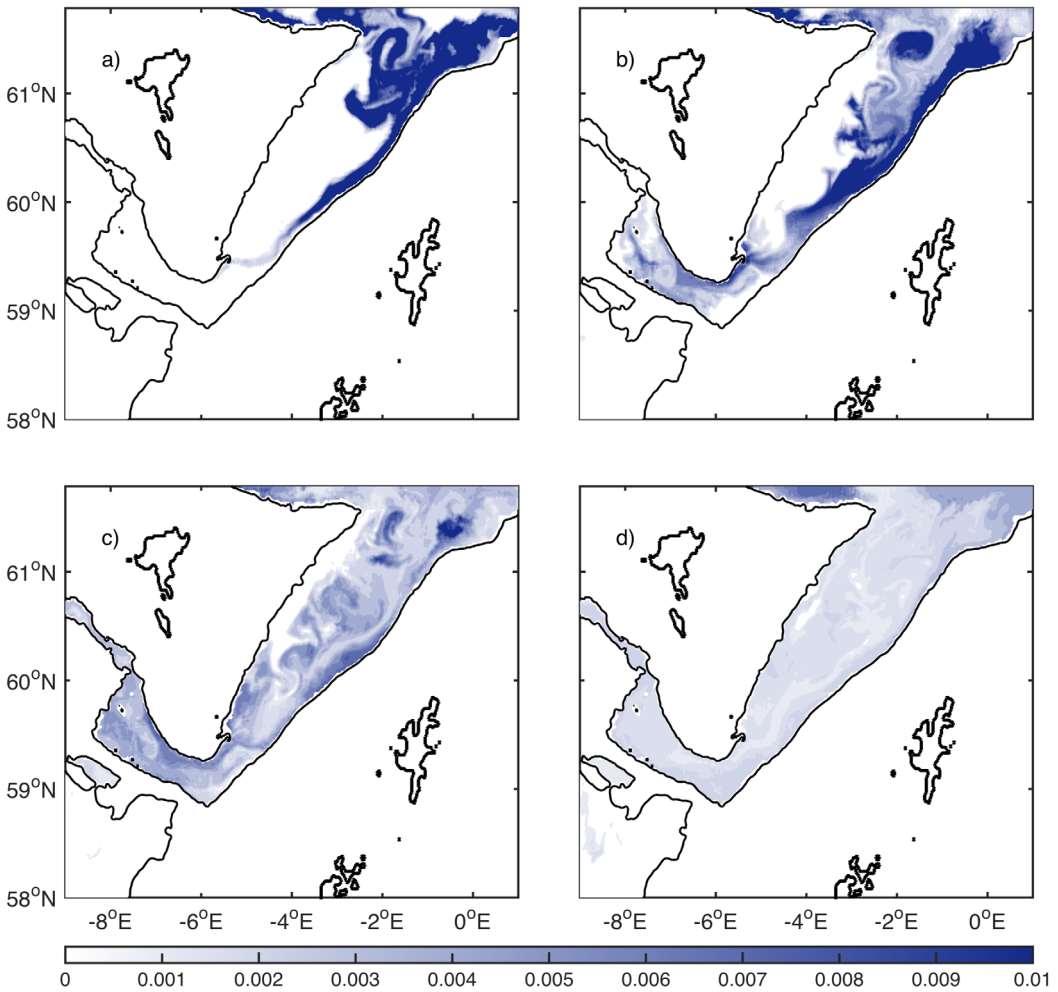

Figure 7. The distribution of the inert tracers (dyes) on the isosurface at 750 m depth (black contours) after (a) 30 days, (b) 60 days, (c) 90 days, and (d) 120 days after release. Land is contoured black for reference.

4. Discussion

The present study investigates the structure of the deep circulation in the FSC though float and tracer release experiments. Persistent eddies alter the flow significantly. They appear to be generated by the channel bathymetry, as they are coincidental with valleys in the sea floor and regions where the flow is forced around the continental shelf or into the shallowing funnel of the channel mouth. Frictional processes at the bottom and shelf slopes coupled with the increasing current speed as the water is squeezed into a shallower, narrower space create a vortex that deflects the slope current at the southern end of the channel whereas the two vortices that occupy the north of the channel form over the deepest valley and against a bend in the Shetland slope. The reason why those eddies may not exist in other models may be that the topography needs to be highly resolved in order to generate those eddies. If the topography is at coarser resolution, the features that are necessary to direct the flow into a vortex are not present and the currents flow uniformly south-eastward. The cartoon in Figure 9 shows the revised picture of the main branches of the deep circulation as established by the model experiments in the present study. Near the Shetland shelf, the deep transport out of the channel is predominantly confined to the fast, narrow current on the slope (solid arrows). The dashed arrows show the northward transport on the Faroese side and key recirculation regions, which are driven by the persistent eddies, are facilitating entrainment and reentrainment of the recirculated waters into the Shetland slope jet.

The failure to find a well-fitting probability distribution function for the distribution density of the float passage time through the channel that encompasses all of the data suggests that the floats must be part of two regimes. Excluding the long, narrow tail of the data set with passage times longer than about 240 days

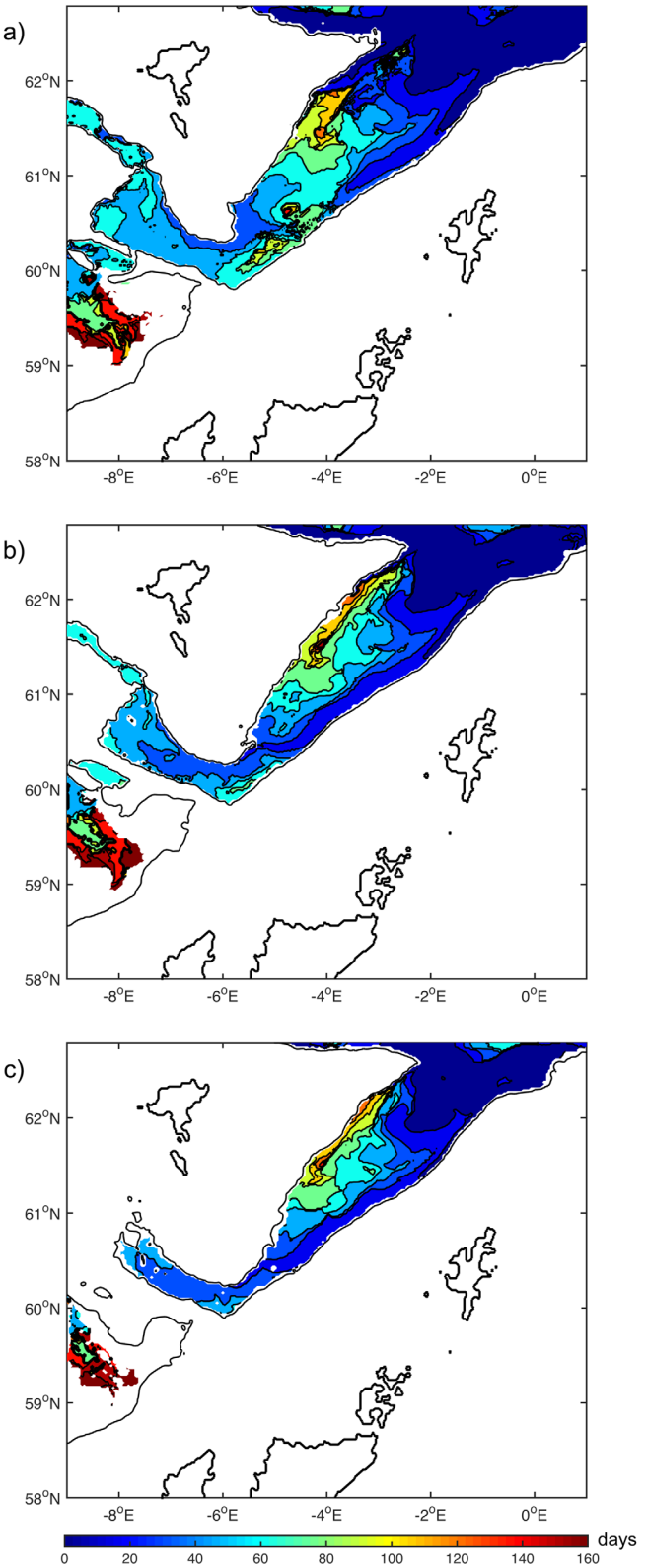

Figure 8. The time it takes for the concentration of the inert tracers (dyes) to first exceed a threshold of 0.001 at (a) 600 m depth, (b) 750 m depth, and (c) 900 m depth. Black contour lines denote the individual depth surfaces and land is contoured black for reference.

allows a significantly better fit of the lognormal probability distribution function and describes the shape and peak of the maximum more accurately. By definition in section 3.2, floats that take longer than 115 days are affected by eddies, which contains all the data in the tail of the full density distribution. Hence two discrete distribution functions are needed in order to describe the data set: one for floats with short passage times within the Shetland slope jet and one for floats which are affected by eddies to varying degrees.

An interesting result of the float experiment is that a significant portion of the floats that enter the FSC return northward and exit the channel to the north near the Shetland shelf slope. In order to do that, the floats would have to cross the fast slope current, which is not possible as the fast flow inhibits cross-jet flow. The northward return of the floats on the Shetland side of the channel can only be achieved if the water masses change their density and become lighter and join the surface waters in doing so. This can also be seen in the map of the time it takes the dye to first reach the threshold concentration at the 600 m depth level. The contours corresponding to the location of the slope jet and the faster threshold times are broken up by contours of threshold times connected to those of the recirculation region closer to the Faroese slope, which suggests the existence of a flow directed toward the Shetland slope across the jet. This result suggests that entrainment and mixing of lighter surface waters must exist within the eddies and allow the depth of the floats to decrease and for the floats to follow shallower currents. However, the ROMS model setup with a third-order upwind horizontal advection scheme is notorious for numerical vertical mixing effects [e.g., *Marchesiello et al.*, 2009]; hence, no attempt is made in this study to quantify diapycnal processes altering the water masses within the deep circulation.

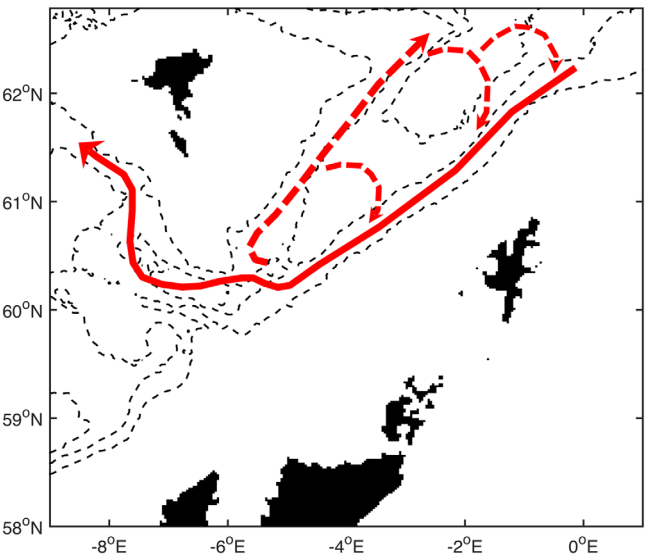

Figure 9. Cartoon showing the main pathways of the deep circulation in the Faroe-Shetland Channel. Model bathymetry below 500 m is shown in dashed contours spaced every 500 m. The red solid arrow denotes the fast current near the Shetland slope and the main pathway of the southwestward volume transport. The red dashed arrows show the northward flow on the Faroese flank where key recirculation regions are indicated by the curved arrows.

Furthermore, the density field and stratification of the model in Figure 3 shows that intermediate water masses are found deeper in the model than they are in reality, which potentially arises from the weaker than observed deep currents in the SODA boundary forcing (not shown here). Slower deep flow in the model (see Figure 4) facilitates less transport of the denser water masses from the north and results in the existence of less of the deepest water masses than in reality and more light and intermediate waters. This effect could partly explain why some floats return northward but it does not exclude numerical effects.

Eddies in the FBC have been identified as mechanisms for modification of the overflow waters, most recently in a modeling/laboratory study by *Cuthbertson et al.* [2014] but those processes within the deep FSC itself have until now not been studied on the larger scale. Our results from the float and tracer release experiments show clearly a significant impact on the composition and transit time of the outflow waters from the existence of persistent topographic eddies. Those eddies change the pathways of the deep currents by lateral redistribution of water masses and recirculation processes. This potentially has implications for the driving mechanisms of the North Atlantic Meridional Circulation and could also be important for climate change factors, such as the transport of dissolved atmospheric CO_2 into the deep ocean.

5. Conclusions

An investigation into the deep circulation of the overflow waters in the Faroe-Shetland Channel has been carried out using a high-resolution regional ocean model. Results from float and tracer release experiments reveal that the mean currents below about 500 m are not directed uniformly to the southwest but have a significantly more complex horizontal structure than previously thought. A fast, narrow current on the slope of the Shetland shelf is the main pathway for the southwestward transport of deep waters from the Nordic seas. Over the rest of the deep interior to the west of this current, persistent topographically generated eddies force the water to recirculate within the channel, subject it to significant amounts of lateral and probably diapycnal mixing and to eventually join the slope current and exit into the FBC or overflow across the Wyville-Thomson Ridge. The northward branch of the deep flow in the model opposes the currently accepted picture of the deep circulation in the FSC but is in agreement with ADCP observations. Our result suggests that during their passage through the FSC, the deep water masses are subject to severe modification by eddies through recirculation and potentially mixing and entrainment.

This study has only investigated the lateral redistribution and recirculation of water masses by the topographic eddies on a larger temporal and spatial scale than typical mixing processes due to the numerical limitations of the model. Some water masses are probably subject to intense diapycnal mixing within the eddies in the channel, which cannot be resolved in the current model setup. Hence, there is scope for continuing this investigation by considering diapycnal processes, such as vertical mixing by the vortices and also by internal waves and tides, that may facilitate a significant amount of interaction between the Atlantic inflow and outflow of deep water though the FSC. Furthermore, no seasonal or tidal dependence of the pathways of the water masses have been investigated, which could also be deciding factors in modifying

the residence time of deep water within the channel as the strength and structure of the eddies and the slope current is likely to fluctuate.

Appendix A: Method and Uncertainty of Calculating the Drain Time

The range of the drain times corresponding to the transport estimates cannot be calculated easily with conventional error analysis methods. One of the main reasons for this is the error in estimating the volume of the FSC below the 3°C isotherm, which varies throughout the channel with minimum depths near the Shetland shelf and sloping down toward the Faroe Plateau. *Hansen and Østerhus* [2007] show that the depth of the isotherm varies between about 400 and 650 m across the FBC. For the experiment in this paper, a mean depth of 550 m is chosen. Due to the nature of the channel bathymetry, the volume uncertainty is incorporated into the drain time experimentally by raising and lowering the isobath by 100 m in the calculation. The error estimate provided by the authors (if available) is incorporated in the same way; hence, an upper and lower limit of the drain time can be determined, which is shown in Table 1. Another source of error, which is difficult to quantify in this experiment is the northern boundary of the FBC. Here the release site of the floats constitutes the northern boundary in order to allow comparison with the float passage time and is also a natural location where the local bathymetry begins to show a "funneling" into the channel. The observations obviously do not require this boundary in determining the FBC transport, hence moving the boundary further north or south would add to the range in estimated drain time.

Acknowledgments

This work was funded by the BP Environmental Technology Program and the Natural Environmental Research Council. The ADCP data were obtained from the Faroese Fisheries Laboratory (contact: Bogi Hansen, bogihan@frs.fo). The authors would like to thank the reviewers, Bee Berx, and one anonymous reviewer, whose comments helped to improve this study.

References

Berx, B., B. Hansen, S. Østerhus, K. M. Larsen, T. Sherwin, and K. Jochumsen (2013), Combining in situ measurements and altimetry to estimate volume, heat and salt transport variability through the Faroe–Shetland Channel, *Ocean Sci.*, *9*(4), 639–654, doi:10.5194/os-9–639-2013.

Borenäs, K. M., and P. A. Lundberg (1988), On the deep-water flow through the Faroe Bank Channel, *J. Geophys. Res.*, *93*(C2), 1281–1292.

Carton, J. A., G. Chepurin, X. Cao, and B. Giese (2000), A simple ocean data assimilation analysis of the global upper ocean 1950–95. Part i: Methodology, *J. Phys. Oceanogr.*, *30*(2), 294–309, doi:10.1175/1520-0485(2000)030<0294:ASODAA>2.0.CO;2.

Cuthbertson, A., P. Davies, N. Stashchuk, and V. Vlasenko (2014), Model studies of dense water overflows in the Faroese Channels, *Ocean Dyn.*, *64*(2), 273–292.

Dooley, H., and J. Meincke (1981), Circulation and water masses in the Faroese Channels during Overflow '73, *Dtsch. Hydrogr. Z.*, *34*(2), 41–55, doi:10.1007/BF02226585.

Haidvogel, D., et al. (2008), Ocean forecasting in terrain-following coordinates: Formulation and skill assessment of the Regional Ocean Modeling System, *J. Comput. Phys.*, *227*(7), 3595–3624, doi:10.1016/j.jcp.2007.06.016.

Hansen, B., and S. Østerhus (2000), North Atlantic–Nordic Seas exchanges, *Prog. Oceanogr.*, *45*(2), 109–208, doi:10.1016/S0079–6611(99)00052-X.

Hansen, B., and S. Østerhus (2007), Faroe Bank Channel overflow 1995–2005, *Prog. Oceanogr.*, *75*(4), 817–856, doi:10.1016/j.pocean.2007.09.004.

Hughes, S. L., W. R. Turrell, B. Hansen, and S. Østerhus (2005), Long term measurements of currents in the Faroe Shetland Channel (1994–2002), *FRS Collab. Rep. 01/05*, Scottish Executive Fisheries Research Services, Aberdeen, U. K.

Larsen, K. M., B. Hansen, and R. Kristiansen (2000), Faroese gem ADCP deployments 1999–2000, *Faroese Fish. Lab. Tech. Rep. 00–02*, Faroe Marine Research Institute, Tórshavn, Faroe Islands.

Larsen, K. M., B. Hansen, E. Mortensen, and R. Kristiansen (2012), Faroese standard sections 1988 - 2010, *Tech. Rep. 12-02*, Havstovan, Faroe Marine Research Institute, Tórshavn, Faroe Islands.

Marchesiello, P., L. Debreu, and X. Couvelard (2009), Spurious diapycnal mixing in terrain-following coordinate models: The problem and a solution, *Ocean Modell.*, *26*, 156–169, doi:10.1016/j.ocemod.2008.09.004.

Mauritzen, C., J. Price, T. Sanford, and D. Torres (2005), Circulation and mixing in the Faroese Channels, *Deep Sea Res., Part I*, *52*(6), 883–913, doi:10.1016/j.dsr.2004.11.018.

Olsen, S. M., B. Hansen, D. Quadfasel, and S. Osterhus (2008), Observed and modelled stability of overflow across the Greenland–Scotland Ridge, *Nature*, *455*(7212), 519–522.

Østerhus, S., B. Hansen, R. Kristiansen, and P. Lundberg (1999), The overflow through the Faroe Bank Channel, *Int. WOCE Newsl.*, *35*, 35–37.

Saha, S., et al. (2010), The NCEP Climate Forecast System Reanalysis, *Bull. Am. Meteorol. Soc.*, *91*(8), 1015–1057, doi:10.1175/2010BAMS3001.1.

Saunders, P. M. (1990), Cold outflow from the Faroe Bank Channel, *J. Phys. Oceanogr.*, *20*(1), 29–43, doi:10.1175/1520-0485(1990)020<0029:COFTFB>2.0.CO;2.

Shchepetkin, A. F., and J. C. McWilliams (2005), The regional oceanic modeling system (ROMS): A split-explicit, free-surface, topography-following-coordinate oceanic model, *Ocean Modell.*, *9*(4), 347–404, doi:10.1016/j.ocemod.2004.08.002.

Shchepetkin, A. F., and J. C. McWilliams (2009), Correction and commentary for "Ocean forecasting in terrain-following coordinates: Formulation and skill assessment of the regional ocean modeling system" by Haidvogel et al., J. Comput. Phys., 227, 3595–3624, *J. Comput. Phys.*, *228*(24), 8985–9000, doi:10.1016/j.jcp.2009.09.002.

Sherwin, T. J., M. O. Williams, W. R. Turrell, S. L. Hughes, and P. I. Miller (2006), A description and analysis of mesoscale variability in the Färoe-Shetland Channel, *J. Geophys. Res.*, *111*, C03003, doi:10.1029/2005JC002867.

Sherwin, T. J., C. R. Griffiths, M. E. Inall, and W. R. Turrell (2008), Quantifying the overflow across the Wyville Thomson Ridge into the Rockall Trough, *Deep Sea Res., Part I*, *55*(4), 396–404, doi:10.1016/j.dsr.2007.12.006.

Smagorinsky, J. (1963), General circulation experiments with the primitive equations I. The basic experiment, *Mon. Weather Rev.*, *91*(3), 99–164, doi:10.1175/1520-0493(1963)091<0099:GCEWTP>2.3.CO;2.

Smith, W. H. F., and D. T. Sandwell (1997), Global sea floor topography from satellite altimetry and ship depth soundings, *Science*, *277*(5334), 1956–962, doi:10.1126/science.277.5334.1956.

Turrell, W. R., G. Slesser, R. D. Adams, R. Payne, and P. A. Gillibrand (1999), Decadal variability in the composition of Faroe Shetland Channel bottom water, *Deep Sea Res., Part I*, *46*(1), 1–25, doi:10.1016/S0967-0637(98)00067-3.

Warner, J. C., C. R. Sherwood, H. G. Arango, and R. P. Signell (2005), Performance of four turbulence closure models implemented using a generic length scale method, *Ocean Modell.*, *8*(1–2), 81–113, doi:10.1016/j.ocemod.2003.12.003.